

An initial study to quantify the resolution difference between an industry leading-edge migration, RTM, and the first migration method that is equally effective at all frequencies at the target

Qiang Fu, Yanglei Zou, and Arthur B. Weglein, M-OSRP/Physics Dept./University of Houston

SUMMARY

There is an industry-wide interest in acquiring lower-frequency seismic data. There are industry reports that (1) when comparing the new and more expensively acquired broad-band lower-frequency data with conventional recorded data, taken over a same region, these two data sets have the expected difference in frequency spectrum and appearance, but (2) they often provide less than the hoped for difference in structural improvement or added benefit for amplitude analysis at the target and reservoir. There are two objectives of this paper: (1) to demonstrate that all current migration and migration-inversion methods (the methods that take recorded data and determine structure and perform amplitude analysis, respectively) make high-frequency asymptotic assumptions and consequently, in the process of migration, they lose or discount the information in the newly-acquired lowest-frequency components in the broad-band data, and (2) to address that problem, with the first migration method that will be equally effective at all frequencies at the target and reservoir, and that will allow the broad-band lower-frequency data to provide greater structural resolution improvement and enhanced amplitude analysis. In this paper, we begin to quantify the difference and the impact on resolution. We provide the first direct comparison of structural resolution differences with data with and without low frequencies, using the same homogeneous velocity model, comparing the current leading edge RTM (Claerbout II imaging principle) and the Stolt extended Claerbout III imaging principle. The new imaging method is able to benefit from broadband data for structural resolution improvement to a much greater extent than the current best industry standard migration. The differences in resolution benefit derived from the Stolt extended Claerbout III migration will be greater when both imaging principle and wave propagation model are included than we report here for only the imaging principle differences.

INTRODUCTION

Migration methods that use wave theory for seismic imaging have two components: (1) a wave-propagation model and (2) an imaging condition. We examine each of these two components with focus on the specific topic of this paper: the frequency fidelity of migration algorithms. That analysis leads to a new and first migration that is equally effective at all frequencies at the target and/or the reservoir. Weglein (2016) provides a detailed development of this new migration method.

For the imaging principle component, a good start is Jon Claerbout's 1971 landmark contribution (Claerbout, 1971) which lists three imaging principles. The first is the exploding-reflector model for stacked or zero-offset data, which we call Claerbout imaging principle I (CI). The second is time-space coincidence of upgoing and downgoing waves, which we call Claerbout

imaging principle II (CII). Waves propagate down from the source, are incident on the reflector, and the reflector generates a reflected upgoing wave. According to RTM (CII), the reflector exists at the location in space where the wave that is downward propagating from the source and the wave propagating up from the reflector are at the same place and time. The third is Claerbout imaging principle III (Stolt extended CIII), which starts with surface source and receiver data and predicts what a source and receiver would record inside the earth. Stolt extended CIII then arranges the predicted source and receiver to be coincident and asks for $t = 0$. If the predicted coincident source and receiver experiment at depth is proximal to a reflector one gets a non-zero result at time equals zero.

CII and Stolt extended CIII are of central industry interest today, since we currently process pre-stacked data. RTM (CII) and Stolt extended CIII will produce different results for a separated source and receiver located in a homogeneous half space above a single horizontal reflector. That difference forms a central and key message of this paper.

CII can be expressed in the form

$$I(\vec{x}) = \sum_{\vec{x}_s} \sum_{\omega} S'(\vec{x}_s, \vec{x}, \omega) R(\vec{x}_s, \vec{x}, \omega), \quad (1)$$

where R is the reflection data (for a shot record), run backwards, and S' is the complex conjugate of the source wavefield.

A realization of Stolt extended CIII is Stolt FK migration (Stolt, 1978)

$$\begin{aligned} M^{stolt}(x, z) &= \frac{1}{(2\pi)^3} \iiint d\omega dx_g dx_s dk_{xx} \\ &\times \exp(-i(k_{sz}z + k_{sx}(x - x_s))) \\ &\times \int dk_{gx} \exp(-i(k_{gz}z + k_{gx}(x - x_s))) \\ &\times \int dt \exp(i\omega t) D(x_g, x_s, t). \end{aligned} \quad (2)$$

The weighted sum of recorded data, summed over receivers, basically predicts the receiver experiment at depth, for a source on the surface. The sum over sources predicts the source in the subsurface. Then the predicted source and receiver experiment is output for a coincident source and receiver, and at time equals zero; it defines a Stolt extended CIII image. Each step (integral) in this Stolt-Fourier form of Stolt extended CIII has a specific physically interpretable purpose towards the Stolt extended CIII image.

RTM IS A HIGH-FREQUENCY APPROXIMATION

Today all migration methods assume a high-frequency approximation in a wave-propagation model or an imaging condition or both. How does one know if a migration method has made

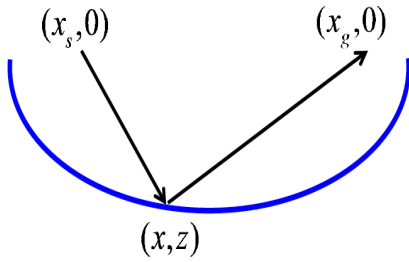


Figure 1: For example, if within a migration method, and focusing on the output of a single trace for a source at $(x_s, 0)$ and a receiver at $(x_g, 0)$ above a single reflector produces a single event that will arrive at time, t_1 . If the migration method output a "ray theory" high frequency approximation for a single event at time t_1 , it will become a set of candidate points (x, y) where $\frac{r_s+r_g}{t_1} = C_0$ where $r_s = \sqrt{(x-x_s)^2 + (y-y_s)^2}$ and $r_g = \sqrt{(x-x_g)^2 + (y-y_g)^2}$

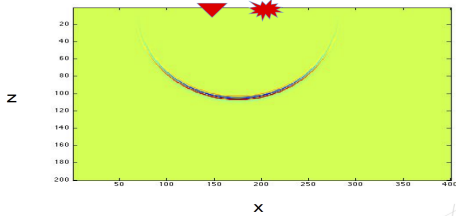


Figure 2: 2D Kirchhoff migration result for one source and one receiver. Kirchhoff is high Frequency approximation from a stationary phase approximation

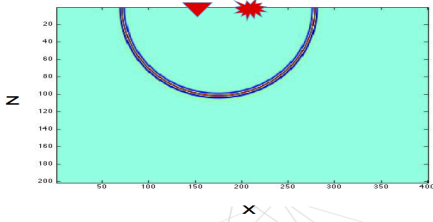


Figure 3: 2D RTM (CII) result for one source and one receiver. There is an intrinsic high frequency assumption within the RTM (CII) imaging principle

a high-frequency approximation? If you have an output shown in Figure 1 (a set of candidate images in the migration process) at any step or stage in the migration method, then the migration method has made an asymptotic high frequency assumption/approximation. If you have a travel time ellipse of candidate images, that's an absolute and definite indication that the migration method has made a high-frequency approximation. This picture (Figure 1) is a ray-theory picture.

In Figure 3 and 4, we compare the results of RTM (CII) and Stolt extended CIII for one source and one receiver, RTM (CII) provides an ellipse while Stolt extended CIII does not. Stolt extended

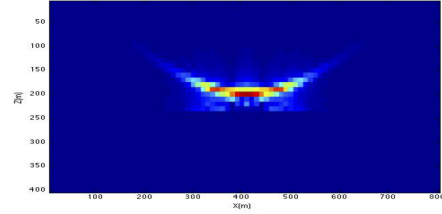


Figure 4: 2D Stolt extended CIII Stolt migration result for one source and one receiver. No high frequency assumption is within the Stolt extended CIII imaging principle

CIII provides a local image. In CII, in this simplest case, where the data is perfect and the medium is homogeneous, the contribution from one source and one receiver, you obtain a set of candidates. Stolt extended CIII will never provide candidates. Stolt extended CIII will bring you to a point in the earth where you have a coincident source and receiver experiment. At time equals zero, if there is a non zero result, you are at a reflector, there is structure there, not a possible or candidate structure. The result from RTM (CII) is a set of candidates of possible structure. That high frequency approximation is intrinsic to Claerbout II, and hence to all the various forms and extensions of RTM.

There are other ways that high frequency approximations can enter migration methods. If you made a stationary phase approximation, the migration method is a high frequency approximation. Kirchhoff migration derives from Stolt extended CIII using a stationary phase approximation and hence is a high frequency approximation (see figure 2). There is another more subtle way that high frequency approximations can enter migration methods. Lets say, we are in Stolt extended CIII (we are predicting the source and receiver experiment at depth) and lets assume a smooth velocity model. If in that smooth velocity model, you were assuming at every point, that the wave is moving in one direction, then you have made a high frequency approximation, even though you are using Stolt extended CIII imaging. The only time that the wave is moving in one direction at a given point is in a homogeneous medium. As soon as you have any deviation from homogeneous, at every point in that medium, part of that wave is moving down and part of wave is moving up. If you are assuming it is only moving in one direction at one point (e.g., using WKBJ or diving waves), you have made a high frequency approximation.

All RTM (CII) imaging, i.e., all RTM methods today are from the imaging principle itself, high frequency approximations/assumptions regardless of how they are implemented. Equation 3 represents a Greens theorem formulation of Stolt extended CIII for one way waves and is equivalent to Stolt migration equation 1. G_0^{-D} is an anticausal Greens function that vanishes on the measurement surface. For a heterogeneous medium assuming one way propagation, at a point (even if you assume it's downgoing and then upgoing, e.g., between source and reflector, and then, separately, first downgoing and then upgoing from reflector to receiver) is a high frequency approximation, even if you are

adopting a Stolt extended CIII imaging principle.

$$P = \int_{S_s} \frac{\partial G_0^{-D}}{\partial z_s} \int_{S_g} \frac{\partial G_0^{-D}}{\partial z_g} P dS_g dS_s \quad (3)$$

Prestack Stolt migration (Green, 1-way waves)

Equation 4 is the new migration method of this paper and we label it Stolt extended Claerbout III for a heterogeneous medium.

$$P = \int_{S_s} \left[\frac{\partial G_0^{DN}}{\partial z_s} \int_{S_g} \left\{ \frac{\partial G_0^{DN}}{\partial z_g} P + \frac{\partial P}{\partial z_g} G_0^{DN} \right\} dS_g \right. \\ \left. + G_0^{DN} \frac{\partial}{\partial z_s} \int_{S_g} \left\{ \frac{\partial G_0^{DN}}{\partial z_g} P + \frac{\partial P}{\partial z_g} G_0^{DN} \right\} dS_g \right] dS_s \quad (4)$$

(Green, 2-way waves) for details see Weglein et al. (2011a,b) and F. Liu and Weglein (2014). It is Stolt extended CIII imaging for a heterogeneous medium, that doesn't assume one-way propagation at either a point, or, separately, overall between source and reflector, and, reflector to receiver. G_0^{DN} is the Green's function for the heterogeneous medium that vanishes along with its normal derivative at the lower surface of the migration volume (Weglein et al., 2011b). Equation 4 is the first migration method that makes no high-frequency approximation in a wave-propagation model or an imaging condition for heterogeneous media, i.e., it is equally effective at all frequencies at the target and at the reservoir.

QUANTIFY THE DIFFERENCE AND IMPACT ON RESOLUTION

All migration methods contain two parts: A, propagation model B, imaging principle. Today all migration methods make a high frequency approximation in A or B or both A and B. Our new migration method (equation 4) is the first that makes no high frequency approximation in both A and B for a heterogeneous medium.

To quantify the impact for a band limited impulsive source, we examine the results of different migration methods with different bandwidths of data - we examine the relative reduction of side lobe amplitudes for each migration methods using conventional and band limited data. Side lobes in the data are an expression of the band limited source. The more we expand the low frequency of the spectrum, (1) the smaller the amplitude of side lobes and (2) the closer the side lobes move towards the image. Side lobes in migration results indicate how the migration method is processing low frequency in the data.

NUMERICAL TEST

Two factors may contribute to imaging effectiveness: the imaging principle itself and its implementation. We would like to isolate the impact of the imaging principle itself. We use a velocity model which is as simple as possible to produce the first direct comparison of structural resolution differences with and without low frequency components of the imaging principles

behind current leading edge RTM (CII) and the new imaging method from M-OSRP, Stolt extended CIII for heterogeneous media.

Figure 5 shows the 1.5D two half-space homogeneous velocity model we used in the test.

Figure 6 shows the two wavelets used to generate synthetic data for this test. One of them is a Ricker wavelet with peak frequency is 15Hz to represent a broadband data. And the other one is the same Ricker with a low-cut filtering to represent the data with out low frequencies. (a) The two wavelets in time domain; (b) The amplitude spectra of the two wavelets.



Figure 5: 1.5D two half-space homogeneous velocity model

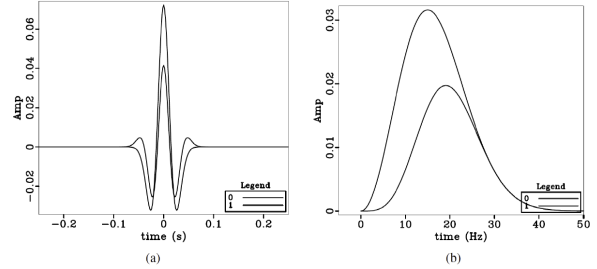


Figure 6: (a) The two wavelets in time domain; (b) The amplitude spectra of the two wavelets.

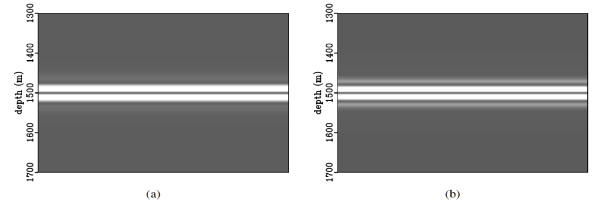


Figure 7: The comparison of (zoomed in) imaging results for both input wavelet by Stolt extended CIII imaging principle. (a) from input data with low frequencies; (b) from input data without low frequencies.

We tested both the input wavelets (with and without low frequencies) on both imaging principles (Stolt extended Claerbout III and Claerbout II). Here we show the results. Figures 7

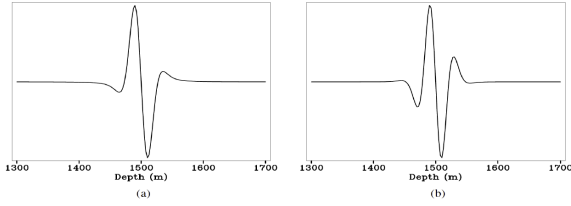


Figure 8: The wiggle comparison of (zoomed in) imaging results for both input wavelet by Claerbout III imaging principle. (a) from input data with low frequencies; (b) from input data without low frequencies. We can measure the normalized amplitudes of the first side lobe for both input data. And it turns out the normalized amplitudes of the first side lobes reduced 57% (from 0.33 to 0.14) if we have low frequencies in the input datas.

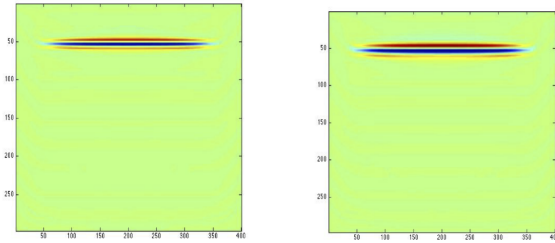


Figure 9: Claerbout II imaging result. (a) for the original data; (b) for the data without low frequency

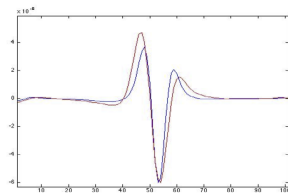


Figure 10: a wiggle comparison of the two images (one trace)

and 8 show the comparison of (zoomed in) imaging results for both input wavelets by Stolt extended CIII imaging principle. In figure 8, we can measure the normalized amplitudes of the first side lobe for both input data. And it turns out the normalized amplitudes of the first side lobes are reduced 57% (from 0.33 to 0.14) if we have low frequencies in the input data. Figures 9 and 10 show the comparison of imaging results for both input wavelets by RTM (CII) imaging principle. In figure 10, the normalized amplitudes of the side lobes are reduced only 21% by including low frequencies, which is much smaller reduction comparing to the Stolt extended CIII results. The fact that RTM (CII) is less able to reduce side lobes with additional low frequency data indicates and quantifies how RTM (CII) is a high frequency approximation and how that property leads to less resolved reflector compared to a Stolt extended CIII migra-

tion. We expect that resolution difference will be significantly greater when the high frequency one-way implementation for heterogeneous medium used in RTM (CII), is compared with the two-way at every point propagation in our new Stolt extended CIII for heterogeneous medium (equation 4).

CONCLUSION

Here we produced the first direct comparison of structural resolution differences with data with and without low frequencies, using the same homogeneous velocity model, comparing the current leading edge RTM (Claerbout II imaging principle) and the Stolt extended CIII migration. There are two factors that contribute to these differences: (1) is the imaging condition itself and (2) the wave propagation model. In current leading-edge migration methods both the imaging condition and the wave propagation model are each separately making high frequency approximations. In the new imaging method from M-OSRP both the imaging condition and method of implementation are equally effective at all frequencies at the target and reservoir (Weglein et al. (2016)). When broadband data is collected over the same area as a conventional bandwidth data, and migrated with the same velocity and algorithm, the data has a different spectrum and shape, but the images at the target and amplitude analysis often show less than the hoped for difference compared to the conventional bandwidth data. There are side lobes in the structural image due to the missing low frequencies. With the new imaging method (Stolt extended CIII for heterogeneous media) and including low frequencies in the input data the side lobes reduced 57% (from 0.33 to 0.14) whereas the conventional leading edge RTM (CII) only reduced the side lobes by 21% (from 0.78 to .62). The new imaging method is able to benefit from broadband data for structural resolution improvement to a much greater extent than the current best industry standard. These tests will continue and will include analysis and comparisons for amplitude analysis. This comparison only tested differences in structural resolution due to the one factor, the imaging condition and focused on a single reflector. Part II of this two part paper, will examine resolution differences for a wedge. The next planned tests will include the wave propagation model for a smooth velocity model. The differences in resolution derived from the new imaging method will be greater when both imaging principle and wave propagation model are included than we report here for only the imaging principle differences.

ACKNOWLEDGMENTS

We would like to thank Dr. Jim Mayhan for his suggestions and help for editing this paper. We are grateful to all M-OSRP sponsors for encouragement and support in this research. We would like to thank all our coworkers for their help in reviewing this paper and valuable discussions.